sciendo

DOI 10.2478/ama-2023-0001

acta mechanica et automatica, vol.17 no.1 (2023)
Special Issue "Machine Modeling and Simulations 2022"

COMPARISON OF VEHICLE SUSPENSION DYNAMIC RESPONSES FOR SIMPLIFIED AND ADVANCED ADJUSTABLE DAMPER MODELS WITH FRICTION, HYSTERESIS AND ACTUATION DELAY FOR DIFFERENT COMFORT-ORIENTED CONTROL STRATEGIES

Zbyszko KLOCKIEWICZ*, Grzegorz ŚLASKI*

*Faculty of Mechanical Engineering, Institute of Machine Design, Poznan University of Technology, ul. Piotrowo 3, 61-138, Poznan, Poland

zbyszko.klockiewicz@put.poznan.pl, grzegorz.slaski@put.poznan.pl

received 1 July 2022, revised 10 August 2022, accepted 11 August 2022

Abstract: Throughout the years, many control strategies for adjustable dampers have been proposed, designed to boost the performance characteristics of a vehicle. Comfort control strategies such as Skyhook (SH), acceleration-driven damping or power-driven damping have been tested many times using simulation models of vehicles. Those tests, however, were carried out using simplified damper models – linear or simple bilinear with symmetric characteristics. This article presents the results of examination of the influence of using more complex damper models, with friction, hysteresis and time delay of state switching implemented, on the chosen dynamic responses of a suspension system for excitations in the typical exploitation frequency range. The results of the test are compared with those found in the literature and with the results of simulations performed with a simplified version of the advanced model used. The main conclusion is that friction and hysteresis add extra force to the already existing damping force, acting like a damping increase for all analysed control strategies. The actuation delays limit the effectiveness in a sense of comfort increasing to only some frequencies. The research shows the importance of including the proposed modules in testing for both adjustable and passive dampers.

Key words: vehicle vertical dynamics, damper model, friction, hysteresis, comfort-oriented control strategies, Skyhook, ADD, PDD

1. INTRODUCTION

The basic task of a suspension system is to ensure safe interactions between vehicle wheels and the road surface while providing satisfactory ride comfort and working in a designed motion range. Oftentimes, satisfying all those needs at once proves impossible [1] as different parameters of suspension elements have different optimal values for safety and comfort. Also, the use of a damper in a typical configuration between sprung and unsprung masses in some situations helps dampen vibrations, while in others, it induces them. The need to change the way in which a damper works in different situations led to the creation of adaptive or semiactive suspension systems. They allow for changing some parameters or switching the damping force during one cycle of vibration. The idea is not new – the patent for adjustable hydraulic shock absorbers was granted in 1957 [2], while control strategies for computer models of vehicles were studied as far back as 1973 [3]. The first widely used control was the comfort-oriented Skyhook (SH) strategy [4], which since then was implemented numerous times in simulations and real-life applications [5–7]. Since then, many more control strategies have been proposed [8], including safety-oriented Groundhook [9], acceleration-driven damper (ADD) [10, 11, 12] and power-driven damper (PDD) [11, 13].

The ADD control strategy minimises the vertical body acceleration (comfort objective) when no road preview is available. Unlike the SH control, the ADD control suppressed the resonance and amplitude in the middle- and high-frequency bands [12]. This strategy uses the same sensors as the SH algorithms and a simple two-state controllable damper.

The PDD control strategy provides results comparable with those of the ADD control strategy, avoiding, at the same time, the chattering effects of the damping control valve [11].

Although much research in that field is conducted purely on theoretical, simplified vehicle models, the real-life implementation of said strategies, while not unseen [14], remains rare. The simplified suspension models use simplified models of damping forces, often utilising the linear damping coefficient [11]. More advanced models include nonlinear characteristics and/or asymmetrical characteristics. In some cases, dry friction is added, while taking damping force hysteresis into account is rare. The same is true for properties connected with damping force adjustment, especially the delay time between the control signal and damping characteristic change.

The authors decided to research into the influence of every additional feature of the damper model on the effectiveness of the damping control strategy in comparison to the model used as the reference model. The subject of research was transfer functions of a quarter car model with different damper models (with internal friction, hysteresis and activation delay implemented) tested with the use of a chirp signal within a frequency range of 0.01–25 Hz.

The present study aims to test the amount of difference in chosen dynamic responses when using a more advanced damper model in simulations, with internal friction, hysteresis and activation delay implemented. Simulations using models with such

features have been carried out before [15, 16]; however, the aim of these models was different from that attempted in this study.

2. RESEARCH METHOD

The current research used computer simulations of a vertical dynamics model of a quarter car implemented in MATLAB/Simulink software. In this research, a set of modified quarter car models with different damper models were used for the different cases of advanced shock absorber models, as presented in Tab. 1.

Tab. 1. Shared features of a quarter car model used in research

Case no.	Nonlinear characteristic	Friction	Hysteresis	Delay
1	✓	-	-	-
2	✓	✓	-	-
3	✓	-	✓	-
4	✓	-	-	✓
5	✓	✓	✓	✓

Case number 1 was chosen as the easiest way to model real damper characteristics as static characteristics. Case numbers 2–5 were also tested in two variants – once without any of the control strategies and once with one of the three tested strategies – SH, ADD or PDD. Other parameters of a suspension were shared between all versions of a model – linear stiffness characteristics of a tire and suspension (Tab. 2).

Tab. 2. Shared features of a quarter car model used in research

Parameter	Unsprung mass	Sprung mass	Tire stiffness	Tire damping	Suspension stiffness
Unit	(kg)	(kg)	(kN/m)	(Ns/m)	(kN/m)
Value	50	400	200	350	30

The tested models were subjected to excitation, enabling the calculation of dynamic responses of suspension in the form of transfer functions between excitation and responses important to the evaluation of the suspension dynamic performance:

- suspension deflection for the evaluation of the necessary rattle space,
- sprung mass acceleration and sprung mass displacement for evaluation of ride comfort, and
- cumulative tire force for the evaluation of safety potential.

The excitation used was a vertical sinusoidal displacement with a constant amplitude of 3 mm, which had variable frequency starting from 0.0001 Hz up to 40 Hz (Fig. 1). The frequency increases were as follows:

1. from 0.0001 to 1 in 100 s – 0.0099 Hz/s,
2. from 1 Hz to 3 Hz in 60 s – 0.0333 Hz/s,
3. from 3 Hz to 10 Hz in 100 s – 0.07 Hz/s and
4. from 10 Hz to 40 Hz in 80 s – 0.375 Hz/s.

Important frequencies when analysing suspension dynamics cover a range from 0.5 Hz to 25 Hz. The frequency values change in a nonlinear fashion in order to allow more cycles in a lower range to occur, which in turn gives better results when calculating transfer functions. Frequencies, both below 0.5 Hz and above 25 Hz, were added to the simulation in order to further stabilise results of the *tfestimate* MATLAB function used to estimate the transfer function of suspension.

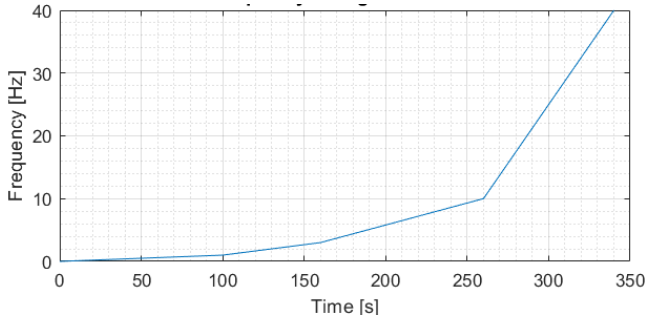

Fig. 1. Changes of the frequency of the input signal over simulation time

2.1. Advanced adjustable damper model

The damper model for all cases, in addition to case no. 1 (labelled as 'linear'), had a nonlinear, asymmetric characteristic, which was identified after empirical testing of damping forces for different levels of control current and averaging these forces to get static characteristics [1], as presented in Fig. 1.

To simplify modelling of the influence of control current on a damping force characteristics, the medium static damping characteristics, between the lowest and the highest, were used as a base characteristic and multiplied by a specific number dependent on the control current and whether the damper was compressed or extended (Fig. 2), resulting in a force that is within the range defined by maximum nonlinear and minimum nonlinear characteristics on the graph. This allowed to model damping forces due to control strategies changing only control current as the input.

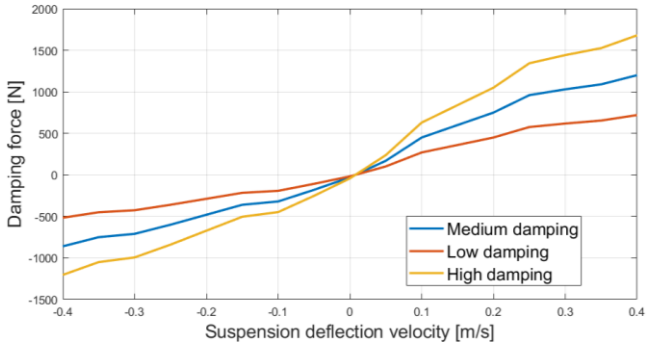

Fig. 2. Damper model static characteristics

All the versions of a damper model, in addition to case no. 1,included a model of an adjustable damper with hysteresis, friction and actuation delay modelled (switched off individually for particular tests). The implementation of this model, based on the study mentioned in Ref [17], was described in the study mentioned in Ref [16] and is shown in Fig. 3.

A total of three main modules to model the total damper force were applied:

DOI 10.2478/ama-2023-0001

– static damping force,
– hysteresis force, and
– friction force.

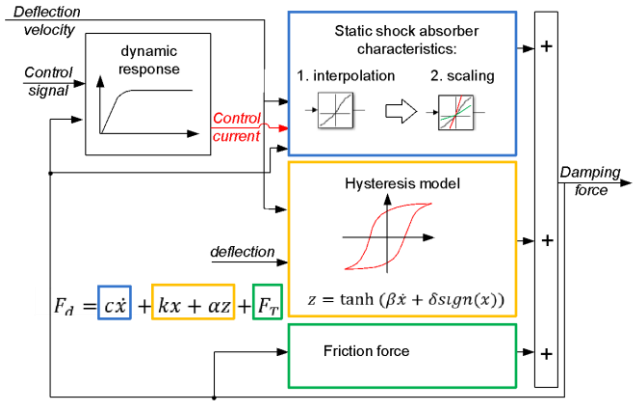

Fig. 3. Damper model diagram

The module generating the biggest forces in the damper model is the static damping characteristics module, which is modelling damping force as a function of deflection speed, differing for the compression and rebound, and also on the control current if it is electrically adjusted damper. For linear and symmetrical characteristics, its damping force can be modelled by simple equations (it was applied for a linear damper for case number 1):

$$F_d = c\dot{x} \tag{1}$$

where c is the damping coefficient and $\dot{x}$ is the damper compression/extension velocity.

In cases of nonlinear and asymmetrical characteristics (in case numbers 2–6), nonlinear equations or interpolation of experimental characteristics can be used. Implementing a damper model in a MATLAB/Simulink software via the lookup table block can be used for the interpolation of the damping force value.

For the adjustable damper, the interpolation is also necessary for the value of damping force in relation to the control current. It too can be carried out with a lookup table block (two-dimensional) for the three-dimensional shock absorber characteristics. In case of a linear relation between control current and damping forces, the medium damping F_{dS_m} static characteristic can be used, and the coefficient to increase or decrease damping force according to the value of valve coil current and state of damper work – compression or rebound:

$$F_{dS\_I} = F_{dS\_m} \cdot K_I \tag{2}$$

where $F_{d\_S\_I}$ is the interpolated value of damping force from static characteristics for given current, F_{dS_m} is the middle static characteristics damping force (for the middle value of valve coil current), and K_I is the coefficient to increase or decrease damping force according to the value of valve coil current and state of damper work – compression or rebound. For modelled shock absorber, formulas for calculating K_I values according to the current value I_c ($0.6 \leq I_c \leq 1.6$ [A]) were determined for compression and rebound, respectively, as follows:

$$\mathrm{K_{IC}} = -0.55\mathrm{I_c} + 1.59 \text{ and } \mathrm{K_{IR}} = -0.71\mathrm{I_c} + 1.74 \tag{3}$$

The Simulink implementation of implementation of Eqs (2) and (3) is presented in Fig. 4.

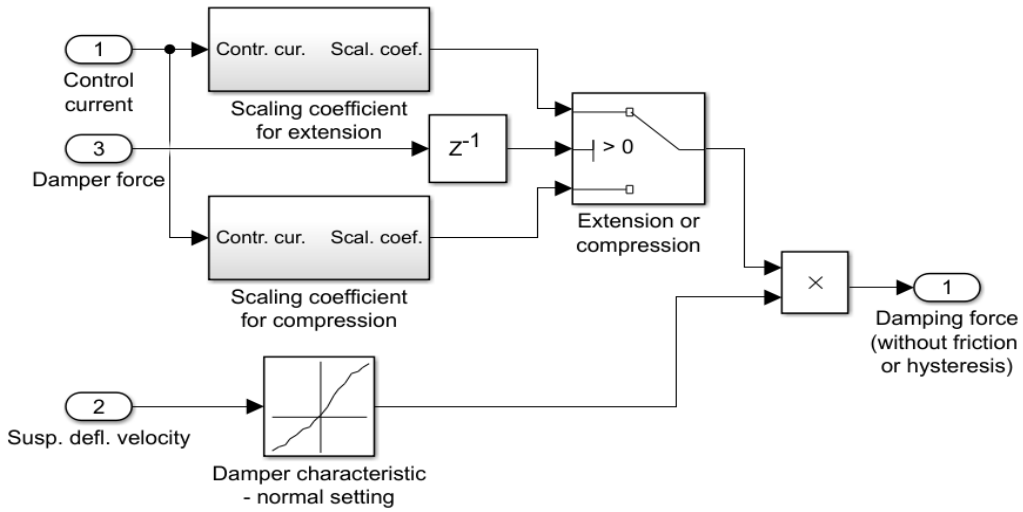

Fig. 4 Damping force calculation subsystem

The damper hysteresis module is important for high damping forces and high velocities. A simple model based on the work mentioned in Ref [6] is proposed to model the hysteretic force–velocity characteristic of the damper. This model is given by the following formulas:

$$F_h = kx + \alpha z \tag{4}$$

$$z = F_0 \cdot tanh\left(\beta\dot{x} + \delta sign(x)\right) \tag{5}$$

where k is the stiffness coefficient which is responsible for the hysteresis opening found from the vicinity of zero velocity; a large value of k corresponds to the hysteresis opening of the ends; z is the hysteretic variable given by the hyperbolic tangent function; β is the scale factor of the damper velocity defining the hysteretic slope, and the large value of β gives a step hysteretic slope; δ is the factor determining the width of the hysteresis through the term δsign(x), a wide hysteresis resulting from a large value of δ; and α

is the scale factor of the hysteresis that determines the height of the hysteresis, and its value depends on the control current.

On the base of an analysis of the dynamic characteristic of tested shock absorber, a formula for the relation between the scale factor α and valve coil current I_C was developed:

$$\alpha = \alpha_0 \cdot (-2.15 I_C + 4.45) \quad (6)$$

where α_0 is the scale factor α of the hysteresis for middle static characteristics damping force.

The hysteresis force value was dependent on both the suspension deflection and its velocity, as well as on the control current value and a number of empirically obtained parameters [19].

The internal friction module is modelling force F_T, and it consists of two elements – the value of kinetic friction force and a signum function due to the model friction force with the opposite sign to the damping force.

The module modelling response time of a shock absorber is based on the model presented in the study mentioned in Refs [7, 8] and consists of two blocks modelling the delay for the damping force increase:

- dead time T_0,
- time delay with a time constant T_Z.

Considering that the time response of tested shock absorbers depends on the stroke direction and the valve operating state, including switching direction (from soft to hard, or vice versa), the four different time delays with use of different values of T_0 and T_Z are calculated in the model and is used according to compression/rebound movement and switching direction. For tested shock absorber, these values were determined to be the same for compression and rebound directions; for switching from soft to hard, they were T_0=4 ms and i T_Z=5 ms, and for switching from hard to soft, T_0=2 ms and i T_Z=3 ms.

This shows that the transfer functions obtained and analysed in the research will not be the same as those in the simpler model, for example, [11]. However, their general course of variability should remain the same with slight changes. The aim of the research designed and presented in this article was to check the qualitative and quantitative influence of taking into account friction, hysteresis and delay time on the transfer function obtained for some comfort-oriented semiactive control strategies for suspension damping.

Lastly, the friction force calculation depended on the suspension deflection velocity; if it was greater than a given threshold, then the friction force had a value equal to defined kinematic friction (35 N), and if it was smaller, then the kinematic friction value was multiplied by a ratio of current suspension deflection velocity to the threshold value (Fig. 1).

$$F_f = \begin{cases} 35 \; if \; v_{defl} > 0.1 \; m/s \\ 35 \cdot \frac{v_{defl}}{0.1} \; if \; v_{defl} < 0.1 \; m/s \end{cases} \quad [N] \quad (7)$$

All the versions of a model that had a control strategy implemented also had a delay module, which caused the current change to occur over a given amount of time. The three modules – friction, hysteresis and delay – could be turned on or off to test their impact on the model behaviour.

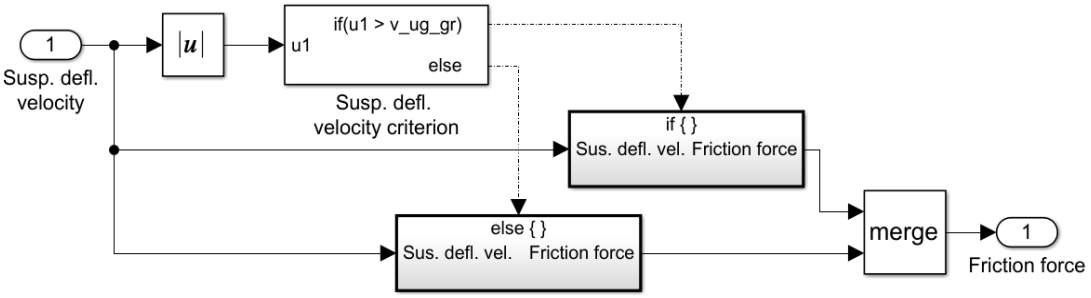

Fig. 5. Friction force calculation subsystem

As stated previously, there were a few versions of a quarter car model; two static versions, one was set to maximum damping force and one with minimum force; and three versions that had different control strategies implemented. The strategies were SH, ADD and PDD. For reference, there were also simplified versions for each of these, which did not have hysteresis, friction or delays, as well as a version with a fully linear characteristic, which was used to determine the influence of previously mentioned modules in the most basic damper model. These three control strategies can be found in many studies, for example, studies given in Refs [6, 7, 11, 19].

3. TESTING AND SIMULATION RESULT ANALYSIS METHODOLOGY

In the cases analysed, a quarter car model was used containing a nonlinear damper model with controllable friction and hysteresis modules, which could be turned on or off. In addition to the damper module, the rest of the model was linear, with the parameters of the model presented in Tab. 2. For each variant, the same excitation was applied – a changing frequency sine wave of amplitude 3 mm, with the course of frequency variability shown in Fig.1.

The influence of implementing friction, hysteresis or both the factors simultaneously was analysed for three indicators – suspension deflections, cumulative force between the tire and the road surface, and sprung mass accelerations for passive dampers and semiactive dampers controlled with different strategies. Analysed indicators allow for the suspension performance evaluation in terms of ride comfort, ride safety and kinematic limitations caused by the finite work range of the suspension.

Because these indicators are not defined by a single value, but rather as a function of frequency, the tool chosen for the analysis was the transfer functions between the given indicator and kinematic excitation.

These functions were calculated using the response signals (deflection, cumulative tire force and sprung mass acceleration) obtained during simulations, as would be performed for a real-life experiments. The transfer functions between these responses and kinematic excitation were then calculated in MATLAB using the *tfestimate* function for the nonlinear, passive model without friction, hysteresis and actuation delay modules, which served as a reference to which results for other variants were then compared to. The reason why these functions were not calculated based on the element characteristics was the nonlinear characteristic of control strategies. The resulting transfer functions were then plotted as graphs, showing their magnitude as the function of frequency, with the range of frequencies from 0.5 Hz to 25 Hz being investigated.

The results for the relative values between a given case and the reference model were represented as bar charts to show the values for four chosen frequencies – near first resonant frequency (ca. 1 Hz), 3 Hz, second resonant frequency (around 10 Hz) and maximum tested frequency 25 Hz.

4. RESULTS

4.1. Influence of friction, hysteresis and actuation delay on the SH strategy

The first tested control strategy that was the SH strategy. The friction and hysteresis affect the work of a damper, as if the damping force increased the, causing the magnitudes for road excitation to suspension deflection transfer function to decrease (Fig. 6).

For transfer functions between road excitation and both cumulative tire force and sprung mass acceleration, friction and hysteresis caused minor changes in the magnitude - dropping by at most 5 % in comparison to reference model. The increase is slightly more significant, especially in the range of 3 to 4 Hz, where friction causes a 10% increase, and the hysteresis contributes to a 20% increase. These values drop significantly, being on par with the reference model for cumulative tire force, while for sprung mass acceleration, after decreasing to around 102%–104% of reference value in the range of 9–10 Hz, it increases again to a maximum tested frequency of 25 Hz. A delay of 30 ms did not have much of an impact on a lower frequency response, as expected. With the growing frequency, its influence increases, which could be observed for sprung mass accelerations and cumulative tire force with the relative increase in magnitude of frequencies in the range of 1.5 Hz to 6 Hz. For suspension deflections, the changes become apparent around 4 Hz value, when relative magnitude starts dropping quickly, reaching 75% for 10 Hz. For higher frequencies it starts going back up, reaching 102% for 25 Hz. The drop in value is visible for other analysed values as well, along with the increase in relative magnitude for values over 10 Hz. Because of the nature of excitation, which is periodical, researchers theorise this behaviour is caused by the fact that the delayed response first starts to act in counterphase to the intended changes, but after reaching a certain threshold, the change from a previous cycle starts to coincide with the next excitation cycle, making the strategy work better. This is supported by a test, in which a 60-ms delay was added, and the results between 30 ms and 60 ms were plotted; it was noticed that for 60 ms, the analogous changes were happening for lower frequencies. The effects of friction, hysteresis and delay combined added up to the total effect in the model with all three being active.

Tab. 3 and Fig. 7 present absolute and relative values of transfer functions of suspension deflection for damper model with the SH control strategy. Frequency ranges chosen for analysis included characteristic frequency bands, such as first and second resonant frequencies or maximal tested frequency.

This way of result presentation was also chosen for the rest of results to minimise number of charts in the article and for easier interpretation of the obtained results.

For the SH control strategy, suspension deflections were mostly influenced by hysteresis for sprung mass resonant frequency and delay in actuation for unsprung mass resonant frequency. Friction had a less impact on transfer function values overall. It can also be noted that all three factors combined caused a larger difference in the transfer function value than the sum of their individual influences. Fig. 8 presents transfer functions between road excitation and cumulative tire force. Tab. 4 and Fig. 9 present absolute and relative values of these transfer functions for the damper model with the SH control strategy.

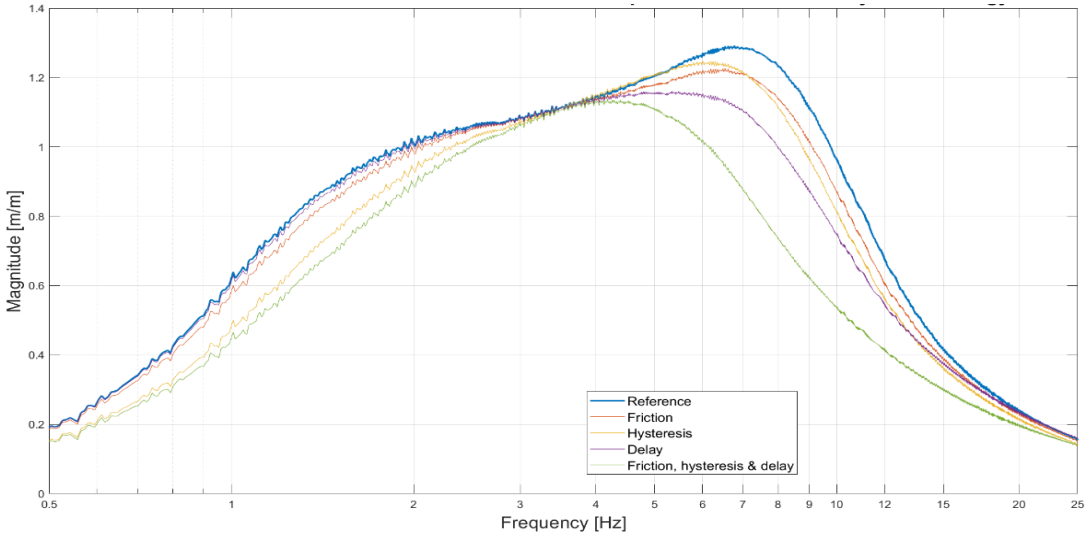

Fig. 6. Transfer functions between kinematic excitation and suspension deflection for the SH (SkyHook) control strategy for advanced and simple damper models. SH, SkyHook

Tab. 3. Absolute values of transfer functions from road excitation to suspension deflection (m/m) for SH, SkyHook

	1st resonant freq. –1 Hz	–3 Hz	2nd resonant freq. –10 Hz	Max. tested freq. 25 Hz
Reference	0.82	1.08	1.15	0.18
Friction	0.77	1.08	1.01	0.18
Hysteresis	0.65	1.07	0.96	0.16
Delay 60 ms	0.8	1.08	0.87	0.19
Fric. + Hyst. + Delay 60 ms	0.6	1.06	0.63	0.16

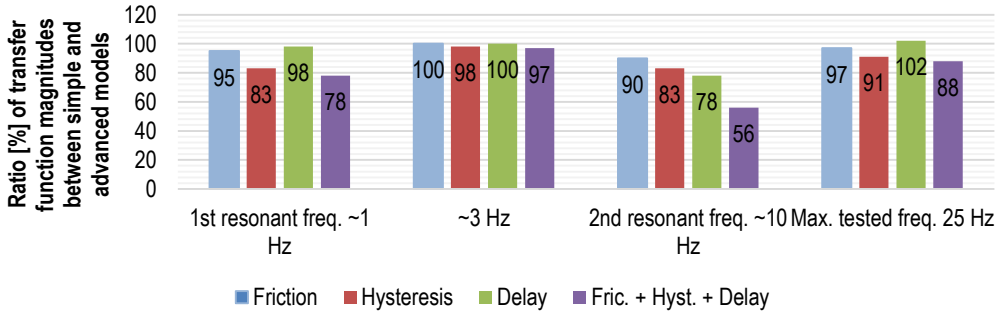

Fig. 7. Relative values of transfer functions from road excitation to suspension deflection of advanced and simple damper models for SH control strategy. SH, SkyHook

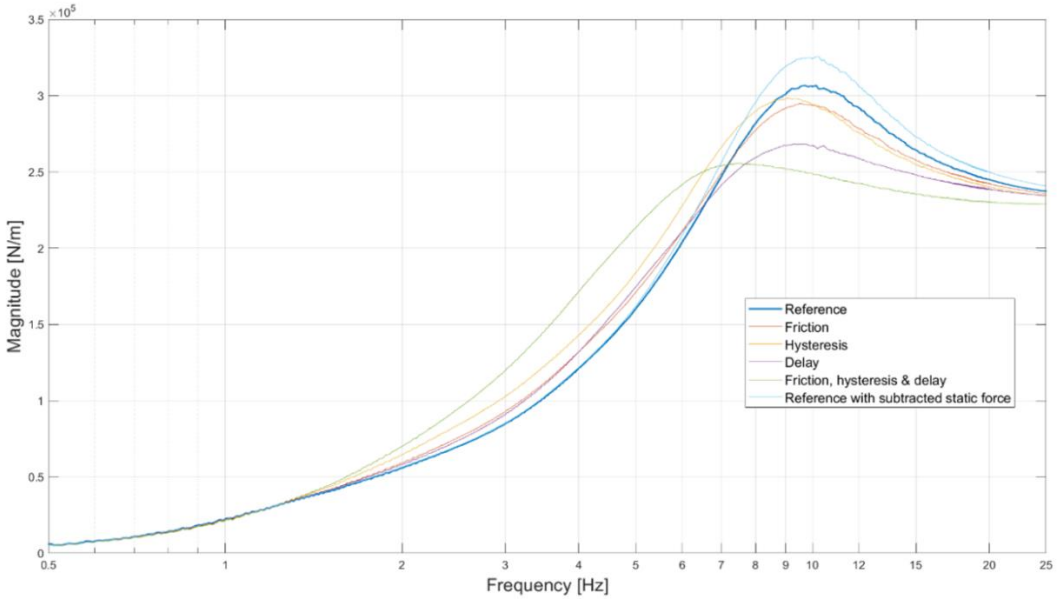

Fig. 8. Transfer functions between kinematic excitation and cumulative tire force for SH control strategy. SH, SkyHook

Tab. 4. Absolute values of transfer functions from road excitation to cumulative tire force (N*10^5/m) for SH, SkyHook

	1st resonant freq. –1 Hz	–3 Hz	2nd resonant freq. –10 Hz	Max. tested freq. 25 Hz
Reference	0.36	0.82	3.05	2.39
Friction	0.37	0.90	2.85	2.38
Hysteresis	0.37	1.03	2.98	2.37
Delay 60 ms	0.37	0.88	2.65	2.37
Fric. + Hyst. + Delay 60 ms	0.37	1.20	2.53	2.30

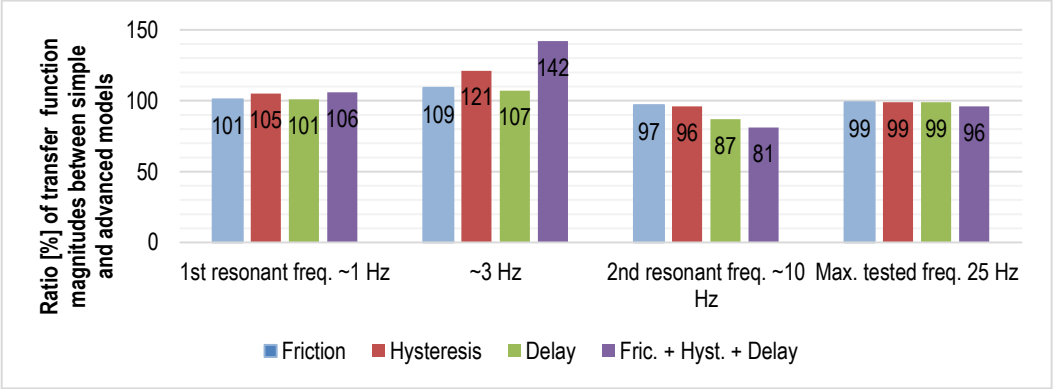

Fig. 9. Relative values of transfer function magnitudes from excitations to tire force cumulative for the SH control strategy and different shock absorber models. SH, SkyHook

Cumulative tire forces for the SH strategy were mostly influenced by hysteresis for 3 Hz and delay for 10 Hz. The highest changes, in general, were seen for the 3 Hz range, where implementation of all three advanced options in the damper model caused the transfer function value to increase by over 40% compared with the reference model; apart from that, for other frequencies, the change was no larger than 13%.

Fig. 10 presents transfer functions between road excitation and sprung mass accelerations, and Tab. 5 and Fig. 11 present absolute and relative values of transfer functions of sprung mass accelerations for the damper model using the SH control strategy. The influence on sprung mass accelerations of all three factors for both resonant frequencies was small, reaching 6% at most; however, it could be much more clearly seen for 3 Hz and 25 Hz. As could be expected, the higher the frequency, more the delay in actuation, contributing to over 30% higher transfer function values.

The influence on sprung mass accelerations of all three factors for both resonant frequencies was small, reaching 6% at most; however, it could be much more clearly seen for 3 Hz and 25 Hz. As could be expected, the higher the frequency, the more delay in actuation of shock absorber valves, contributing to over 30% higher transfer function values.

The increase in magnitudes of transfer functions between road excitation and cumulative tire force and between sprung mass acceleration is significant in the range of 3–4 Hz, where friction causes a 10% increase and hysteresis contributes to a 20% increase. These values drop significantly being on par with the reference model for cumulative tire force, while sprung mass acceleration after decreasing to around 102%–104% of the reference value in the range of 9–10 Hz, they increased again up to a maximum tested frequency of 25 Hz.

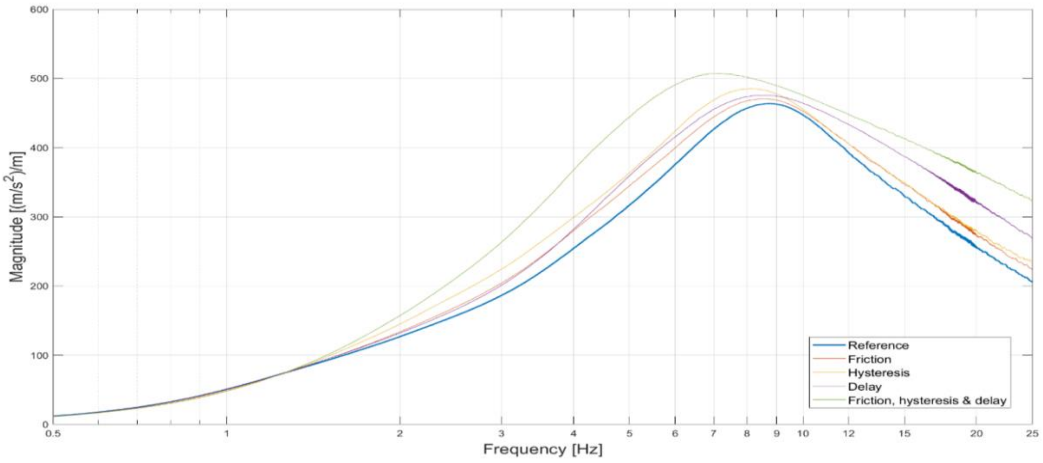

Fig. 10 Transfer functions from kinematic excitation to sprung mass acceleration for the SH control strategy. SH, SkyHook

Tab. 5. Absolute values of transfer functions from road excitation to sprung mass acceleration the for SH control strategy for different damper models

Values in (m/m/s²)	1st resonant freq. –1 Hz	–3 Hz	2nd resonant freq. –10 Hz	Max. tested freq. 25 Hz
Reference	90	190	460	205
Friction	90	205	465	225
Hysteresis	90	230	475	235
Delay 60 ms	90	200	470	270
Fric. + Hyst. + Delay 60 ms	90	265	485	325

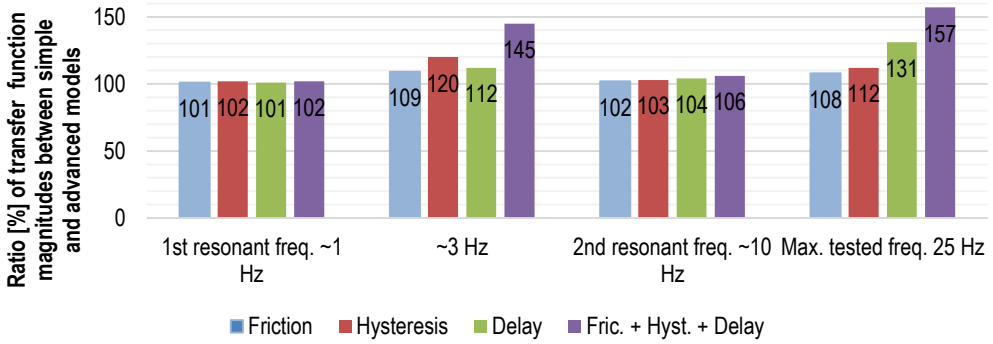

Fig. 11. Relative values of transfer function magnitudes from excitations to sprung mass accelerations for the SH control strategy for different shock absorber models. SH, SkyHook

A delay of 30 ms did not have much of an impact on lower frequency response, as expected. With the growing frequency, its influence increased, which could be observed for sprung mass accelerations and cumulative tire force as the relative increase in magnitude for frequencies in the range of 1.5–6 Hz. For suspension deflections, the changes caused by delay became apparent around 4 Hz value, when relative magnitude started dropping quickly, reaching 75% for 10 Hz, after which frequency it started going back up, reaching 102% for 25 Hz. The drop in value is visible for other analysed values as well, along with the rise in relative magnitude for values over 10 Hz. Because of the nature of excitation, which is periodical, researchers theorise this behaviour is caused by the fact that the delayed response first starts to act in counterphase to the intended changes, but after reaching a certain threshold, the change from a previous cycle starts to coincide with the next excitation cycle, making the strategy work better. This is supported by a test, in which a 60-ms delay was added and the results between 30 ms and 60 ms were plotted; it was noticed that for 60 ms, the analogous changes occurred for lower frequencies. The effects of friction, hysteresis and delay combined once again added up to the total effect in the model, with all three being active.

4.2. Influence of friction, hysteresis and actuation delay on ADD strategy

The second analysed strategy was ADD, and similar patterns emerge when analysing the transfer functions (Fig. 12), with slightly different values.

Tab. 6. and Figs. 12 and 13 present absolute and relative values of transfer functions of suspension deflection for the damper model using the ADD control strategy. In general, the influence of friction and hysteresis was comparable with that of the SH strategy, with the exception of hysteresis having a greater impact on low frequency behaviour, increasing the relative values. Delay, in general, has less impact on the all analysed transfer functions; however, interestingly, it causes a slight increase (3%–4%) in the relative value near the first resonant frequency across the board and also for the second resonant frequency (2%–3%) in case of sprung mass acceleration and cumulative tire force. For suspension deflection, the relative magnitude is lowered by the same amount of around 3%.

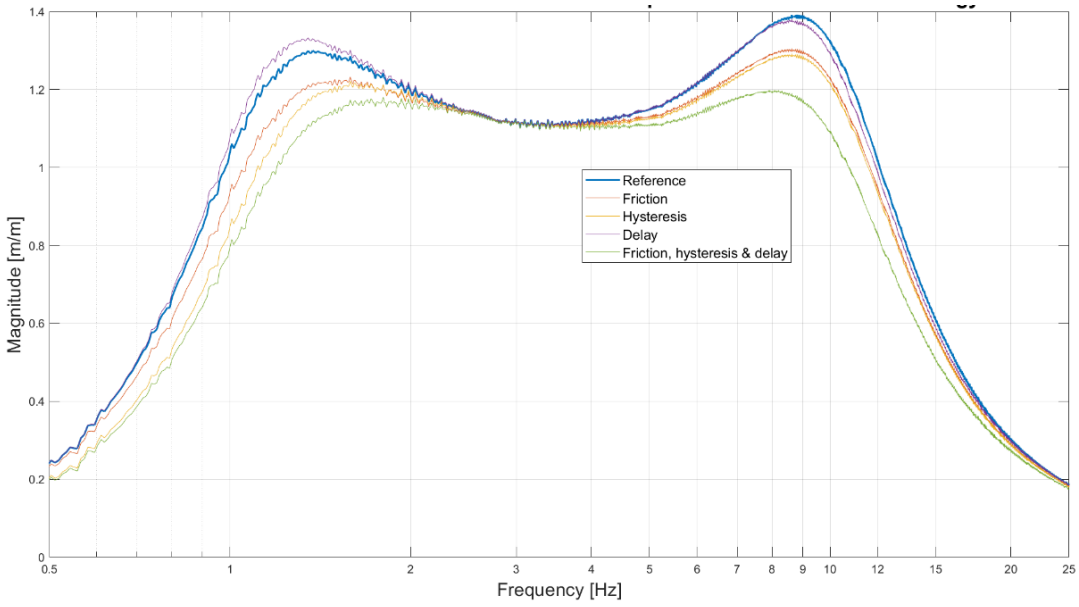

Fig. 12. Transfer functions between kinematic excitation and suspension deflection for the ADD control strategy. ADD, acceleration-driven damper

Tab. 6. Absolute values of transfer functions from road excitation to suspension deflection (m/m) for the ADD control strategy for different damper models

	1st resonant freq. –1 Hz	–3 Hz	2nd resonant freq. –10 Hz	Max. tested freq. 25 Hz
Reference	1.28	1.13	1.39	0.19
Friction	1.22	1.13	1.29	0.19
Hysteresis	1.21	1.13	1.27	0.19
Delay 60 ms	1.33	1.13	1.35	0.19
Fric. + Hyst. + Delay 60 ms	1.15	1.13	1.16	0.18

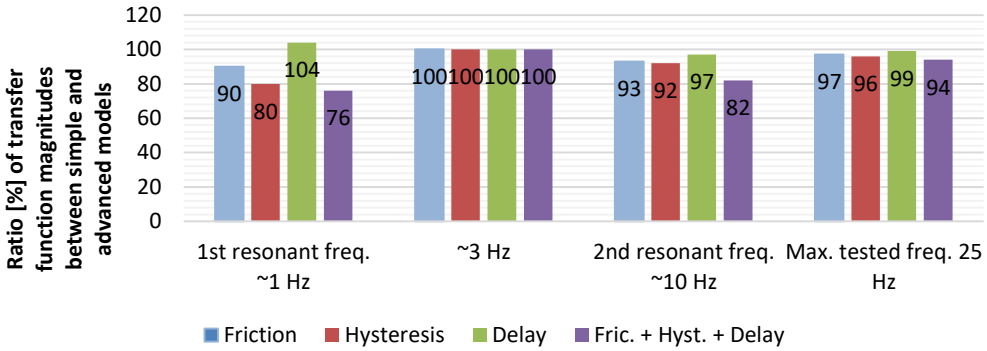

Fig. 13. Relative values of transfer function magnitudes from excitations to suspension deflections for the ADD control strategy for different shock absorber models. ADD, acceleration-driven damper

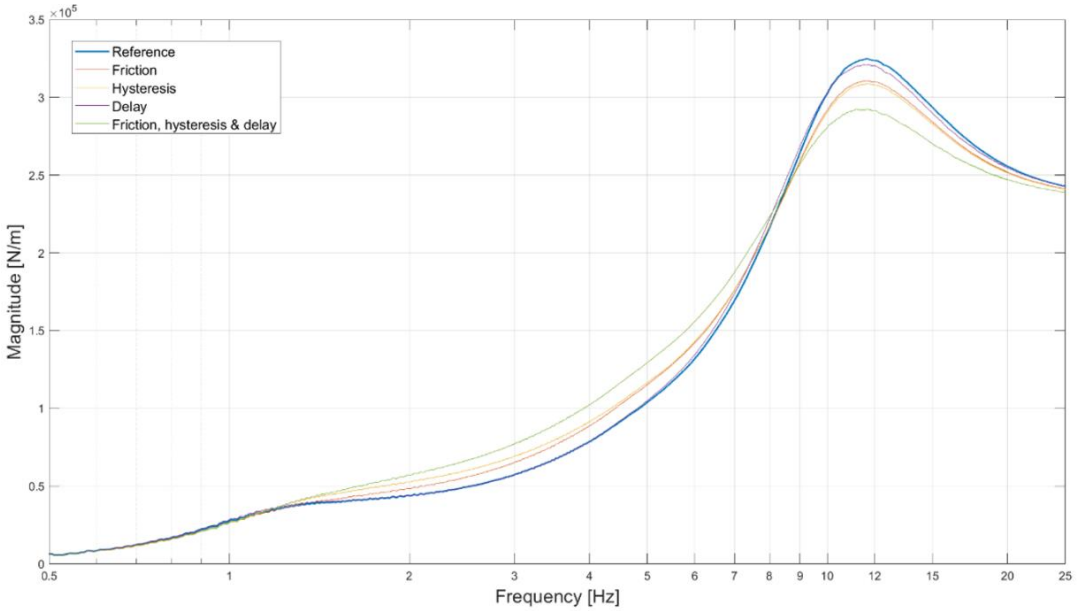

Fig. 14. Transfer functions between kinematic excitation and cumulative tire force for the ADD control strategy. ADD, acceleration-driven damper

Tab. 7. Absolute values of transfer functions between road excitation and cumulative tire force (N*10^5/m) for ADD

	1st resonant freq. –1 Hz	–3 Hz	2nd resonant freq. –10 Hz	Max. tested freq. 25 Hz
Reference	0.37	0.57	3.25	2.43
Friction	0.36	0.67	3.10	2.42
Hysteresis	0.36	0.71	3.09	2.42
Delay 60 ms	0.0.40	0.57	3.22	2.43
Fric. + Hyst. + Delay 60 ms	0.35	0.78	2.90	2.41

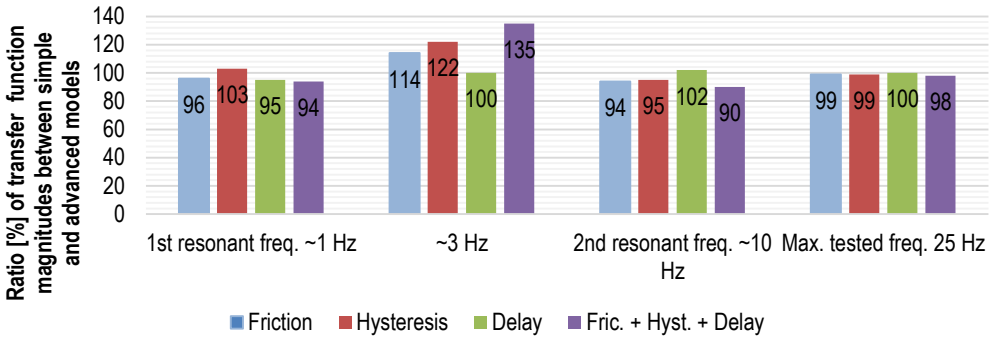

Fig. 15. Relative values of transfer function magnitudes from excitations to cumulative tire force for the ADD control strategy for different shock absorber models. ADD, acceleration-driven damper

The ADD control strategy in case of suspension deflections is less influenced by the addition of damper model elements like friction, hysteresis and especially actuation delay than by the SH control strategy. Friction and hysteresis affect the model behaviour to almost an identical degree, which does not exceed 10%.

Tab. 7 and Fig. 14 present absolute and relative (Fig. 15) values of transfer functions of cumulative tire force for various damper models with the ADD control strategy.

In terms of cumulative tire force, the influence of hysteresis and friction can be seen more clearly, especially for the 3 Hz range. The transfer function values there are around 15% to 20% higher, when these two model elements are added. The actuation delay still does not produce a meaningful change in transfer function values.

Tab. 8 and Fig. 16 present absolute and relative (Fig. 17) values of transfer functions of sprung mass accelerations for the damper model with the ADD control strategy.

Sprung mass accelerations are mostly influenced by hysteresis, followed by friction. Delay once again almost does not influence the results. The highest impact is seen for 3 Hz and 25 Hz as was also the case for the SH control strategy.

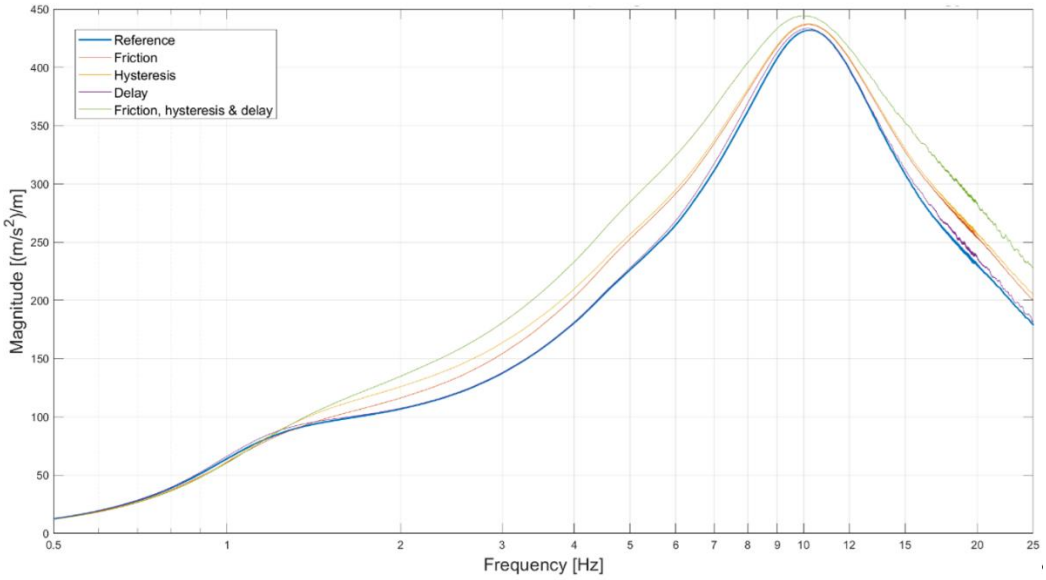

Fig. 16. Transfer functions between kinematic excitation and sprung mass acceleration for the ADD control strategy. ADD, acceleration-driven damper

Tab. 8. Absolute values of transfer functions between road excitation and sprung mass acceleration ([m/s^2]/m) for ADD

	1st resonant freq. –1 Hz	–3 Hz	2nd resonant freq. –10 Hz	Max. tested freq. 25 Hz
Reference	65	135	430	182
Friction	63	155	438	200
Hysteresis	63	168	438	203
Delay 60 ms	66	135	431	185
Fric. + Hyst. + Delay 60 ms	63	180	442	230

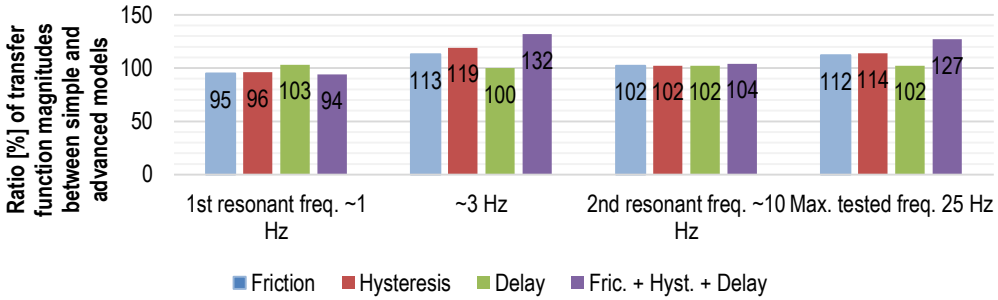

Fig. 17. Relative values of sprung mass accelerations for ADD. ADD, acceleration-driven damper

In general, in a case of the ADD strategy, the influence of friction and hysteresis was comparable with that in the SH strategy, with the exception of hysteresis having a greater impact on low frequency behaviour, increasing the relative values. Delay, in general, has less impact on the all analysed transfer functions; however, interestingly, it causes a slight increase (3%–4%) in the relative value near the first resonant frequency across the board and also for the second resonant frequency (2%–3%) in case of sprung mass acceleration and cumulative tire force. For suspension deflection, the relative magnitude is lowered by the same amount of around 3%.

4.3. Influence of friction, hysteresis and actuation delay the PDD strategy

The last tested control strategy was the PDD strategy. The overall impact of friction and hysteresis on the behaviour of the model was similar to that of the ADD strategy, with hysteresis having relative gain slightly lower by around 12% to 14% points for the first and second resonant frequencies, respectively, for suspension deflection – Tab. 9. Cumulative tire force and sprung mass acceleration functions also have slightly lower relative gains for most frequencies, except for the 3–4 Hz range, where the relative gain is actually higher by around 10% points. Delay functions a bit differently; it has almost no impact on any of the dynamic responses. The cumulative effects of all three are as previously – mostly a sum of individual influences.

The effects of the PDD strategy are similar to those of ADD, with the difference being that in case of PDD, the influence is on average 5%–10% higher for hysteresis, while friction and delay do not change much. The greatest effects are seen for both resonant frequencies.

Tab. 10 and Figs. 20 and 21 present absolute and relative values of transfer functions of cumulative tire force for the damper model with the PDD control strategy.

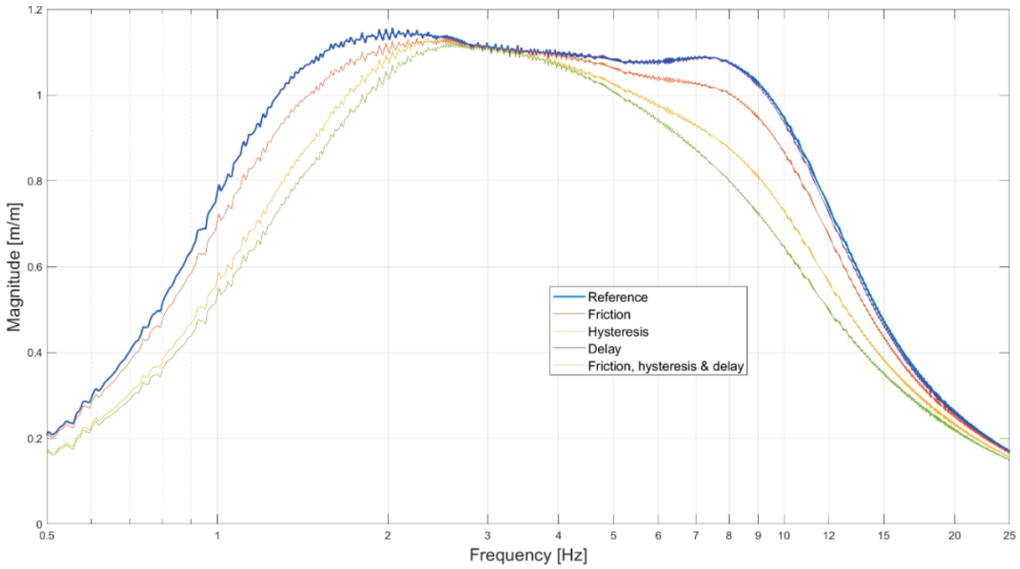

Fig. 18. Transfer functions between kinematic excitation and suspension deflection for the PDD control strategy. PDD, power-driven damper

Tab. 9. Absolute values of transfer functions between road excitation and suspension deflection (m/m) for PDD

	1st resonant freq. –1 Hz	–3 Hz	2nd resonant freq. –10 Hz	Max. tested freq. 25 Hz
Reference	0.78	1.12	1.08	0.17
Friction	0.72	1.12	1.01	0.17
Hysteresis	0.58	1.12	0.88	0.16
Delay 60 ms	0.78	1.12	1.08	0.17
Fric. + Hyst. + Delay 60 ms	0.53	1.12	0.72	0.15

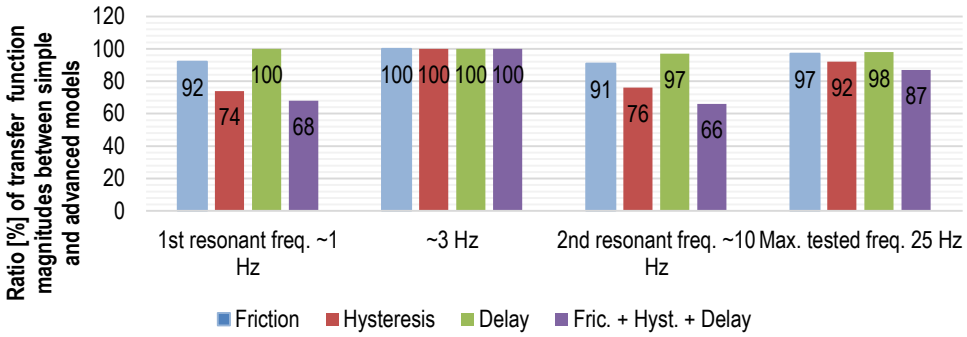

Fig. 19 Relative values of suspension deflections for PDD. PDD, power-driven damper

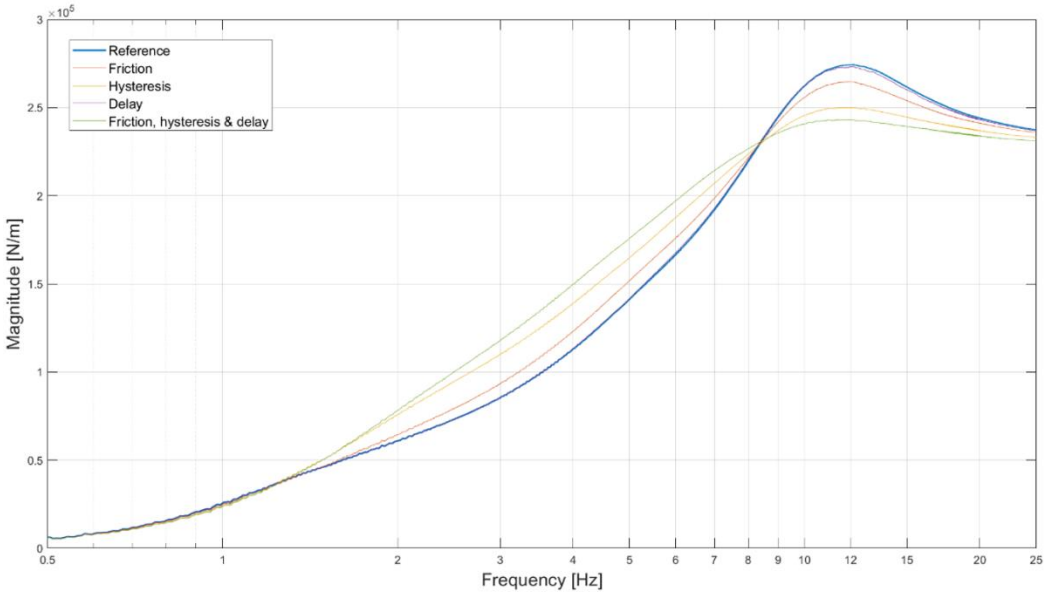

Fig. 20. Transfer functions between kinematic excitation and cumulative tire force for the PDD control strategy. PDD, power-driven damper

Tab. 10. Absolute values of transfer functions between road excitation and cumulative tire force (N*10^5/m) for PDD

	1st resonant freq. –1 Hz	–3 Hz	2nd resonant freq. –10 Hz	Max. tested freq. 25 Hz
Reference	0.42	0.81	2.68	2.34
Friction	0.42	0.91	2.57	2.34
Hysteresis	0.46	1.12	2.50	2.31
Delay 60 ms	0.42	0.81	2.65	2.35
Fric. + Hyst. + Delay 60 ms	0.46	1.20	2.40	2.29

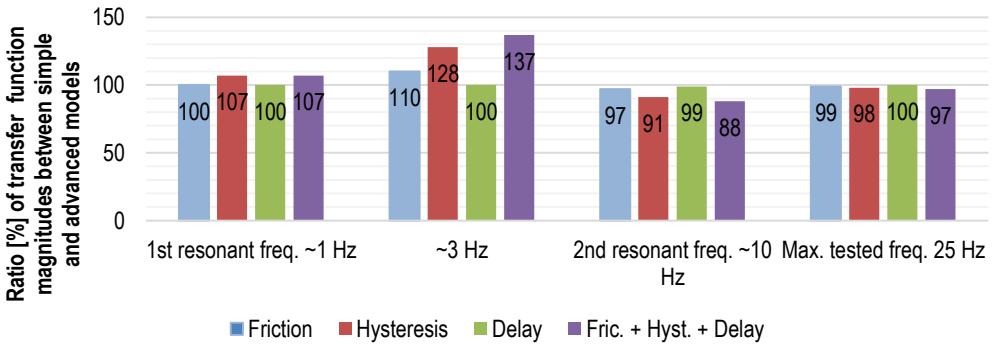

Fig. 21. Relative values of cumulative tire force for PDD. PDD, power-driven damper

Similarly to suspension deflection, the effects on cumulative tire strength are comparable for PDD and ADD strategies. The highest influence is caused by hysteresis, especially for low (1–3 Hz) frequencies, while friction and delay almost do not play a role when it comes to changing transfer function values.

Tab. 11 and Fig. 7 present absolute and relative (Fig. 23) values of transfer functions of sprung mass accelerations for the damper model with the PDD control strategy.

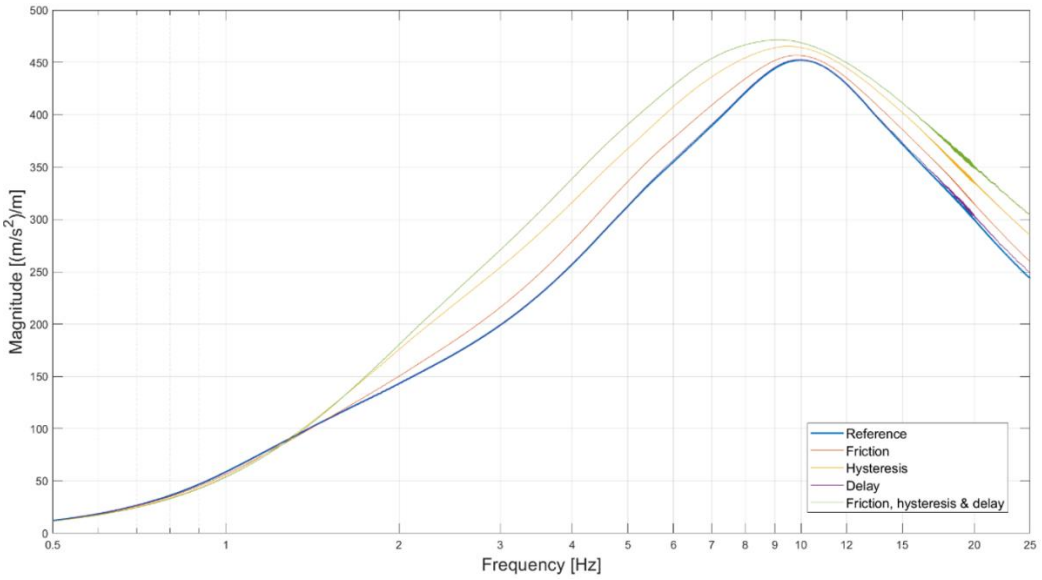

Fig. 22 Transfer functions between kinematic excitation and sprung mass acceleration for the PDD control strategy. PDD, power-driven damper

Tab. 11. Absolute values of transfer functions between road excitation and sprung mass acceleration ([m/s²]/m) for PDD

	1st resonant freq. –1 Hz	–3 Hz	2nd resonant freq. –10 Hz	Max. tested freq. 25 Hz
Reference	60	200	450	248
Friction	58	215	452	260
Hysteresis	57	254	465	285
Delay 60 ms	60	200	442	250
Fric. + Hyst. + Delay 60 ms	56	270	470	305

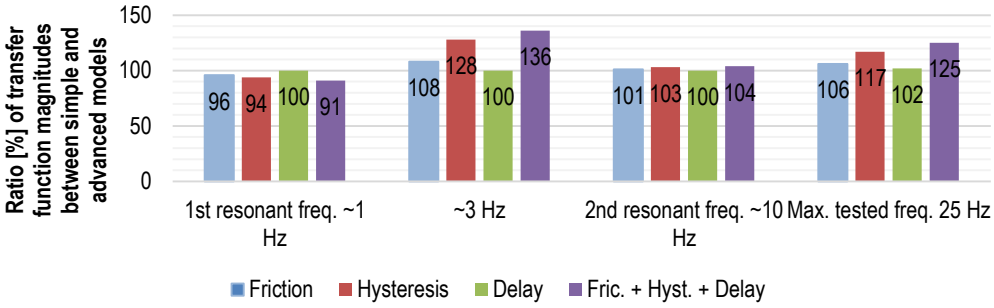

Fig. 23. Relative values of sprung mass accelerations for PDD. PDD, power-driven damper

Sprung mass accelerations are slightly less affected by the advanced damper model elements for the PDD strategy than those for ADD, but the highest influences can yet again be found for 3 Hz and 25 Hz. Hysteresis plays the largest role in transfer function values.

The overall impact of friction and hysteresis on the behaviour of the model controlled by the PDD strategy was similar to that of an ADD strategy, with hysteresis having relative gain slightly lower by around 12%–14% points for the first and second resonant frequencies, respectively, for suspension deflection. Cumulative tire force and sprung mass acceleration functions also have slightly lower relative gains for most frequencies, except for the 3–4 Hz range, where the relative gain is actually higher by around 10% points. Delay functions a bit differently; it has almost no impact on any of the dynamic responses. The cumulative effects of all three are as previously – mostly a sum of individual influences.

5. CONCLUSIONS

In case of simulation testing of the advanced nonlinear model of suspension (stiffness and damping suspension forces con-

trolled by nonlinear strategies), transfer functions have to be calculated using response signals (deflection, cumulative tire force and sprung mass acceleration) obtained during simulations, as would be performed for real-life experiments. After preparing simulated signals in the form of time histories, frequency response evaluation can be made using the quotient of estimator of cross-power spectral density of kinematic excitation signals and suspension responses signals and estimator of power spectral density of kinematic excitation signals. This method can be implemented with the use of ready-to-use software functions used to estimate transfer functions, for example, MATLAB *tfestimate*, which was proved in the present research.

The obtained results allow for formulating the following conclusions about the influence of friction and hysteresis on transfer functions for suspension controlled with various control strategies:

SH: Friction and hysteresis increase the damping force, causing the magnitudes for road excitation to suspension deflection transfer function to decrease. It has a similar effect on transfer functions between road excitation and cumulative tire force, as well as sprung mass acceleration, albeit to a lesser degree.

The decrease in the transfer function of suspension deflection for only friction added is smaller for the range of 1 Hz (5%) than for the 10 Hz range (10%). Friction and hysteresis decrease transfer function magnitude, respectively, about 22% and 44%. In the range of frequencies between sprung mass and unsprang mass resonance (between 1 Hz and 10 Hz) and over unsprung mass resonance (about 25 Hz), the influence of friction and hysteresis is smaller – 3% and 12,% respectively.

The transfer function for tire forces was mostly influenced by hysteresis (for 3 Hz) and delay (for 10 Hz). The greatest increase in the transfer function was seen for the 3 Hz range, where implementation of all models friction, hysteresis and delay increased this function value by about 40% compared with the reference model; apart from that, for other frequencies, the change was no larger than 13%.

Actuation delay makes a little difference for low frequencies, but this influence starts growing once 1 Hz frequency is achieved, peaking around 3 Hz, when it starts to drop again. In addition to changing transfer function values, delay also seems to shift unsprung mass resonant frequency to lower by around 1 Hz.

ADD: The same effects of adding friction and hysteresis to the damper model as in SH case can be observed; they act as if damping force increased. Delay contribution, while acting in the same manner for unsprung mass resonant frequency, actually causes the model to behave like damping force was lower for the sprung mass resonant frequency. In general, compared with other modules, delay plays a much smaller role in the ADD control strategy, contributing to at most 5% change for resonant frequencies for either of analysed dynamic responses. Friction, while mostly having a similar extent of influence on transfer functions, reaches 10% of change in the value for sprung mass resonant frequency in the suspension deflection transfer function. The highest impact on all transfer functions is caused by hysteresis, exceeding 20% in case of tire force.

PDD: Delay has almost no effect on the transfer functions for responses in the PDD control strategy. The effects of friction and hysteresis once again mimic the increase in damping force. Also, similar to the ADD control strategy, hysteresis seems to play a much greater role for all analysed dynamic responses, with even higher relative changes – up to 30% for cumulative tire forces.

The main conclusion is that friction and hysteresis add extra force to the already existing damping force, thus acting as if its value increased for all analysed control strategies. Hysteresis seems to have higher impact than friction for all strategies, reaching up to a 30% relative change (PDD tire force), while friction reaches at most 14% (ADD, also tire force). SH and ADD strategies seem to be mildly affected by implementation of actuation delay, while the PDD strategy remains practically unchanged until 15 Hz, where slight changes (no more than 2% relative value) can be observed for some of the transfer functions. Its importance can potentially be higher, if the actuation delay is >60 ms.

The research shows the importance of including proposed modules in testing for both adjustable and passive dampers. The combined effects of all three modules often exceed a 40% relative value change, which might lead to greatly overestimated gains from implying such theoretically beneficial control strategies. The inclusion of friction and hysteresis in the equations defining the strategies, to offset their real-life effects on stiffening suspension, might yield positive results. As for the effects of actuation delay, its influence might be diminished by developing forward scanning sensors, which could prepare suspension for upcoming excitations in advance.

REFERENCES

1. Els PS, Theron NJ, Uys PE, Thoresson MJ. The ride comfort vs. handling compromise for off-road vehicles. J. Terramechanics, 2007;44(4):303–317.
2. Sturari C, Adjustable shock absorber, US2780321A, 1957.
3. Yue C. Control law designs for active suspensions in automotive vehicles, 1988.
4. Crosby MJ, Karnopp DC. The Active Damper—A New Concept for Shock and Vibration Control. Shock Vib. Bull. 1973;43:119–133
5. Emura J, Kakizaki S, Yamaoka F, Nakamura M. Development of the Semi-Active Suspension System Based on the Sky-Hook Damper Theory. J. Passeng. CARS. 1994;103:1110–1119.
6. Hong KS, Sohn HC, Hedrick JK. Modified Skyhook Control of Semi-Active Suspensions: A New Model, Gain Scheduling. and Hardware-in-the-Loop Tuning. J. Dyn. Syst. Meas. Control, 2002;124(1): 158–167.
7. Savaresi SM, Spelta C. Mixed Sky-Hook and ADD: Approaching the Filtering Limits of a Semi-Active Suspension. J. Dyn. Syst. Meas. Control. 2007;129(4):382–392
8. Ślaski G. Studium projektowania zawieszeń samochodowych o zmiennym tłumieniu. Poznań: Wydawnictwo Politechniki Poznańskiej, 2012.
9. Valášek M, Novák M, Šika Z, Vaculín O. Extended ground-hook – New concept of semi-active control of truck's suspension. Veh. Syst. Dyn. 1997;27(5-6):289–303.
10. Savaresi SM, Silani E, Bittanti S. Acceleration-Driven-Damper (ADD): An Optimal Control Algorithm For Comfort-Oriented Semiactive Suspensions. J. Dyn. Syst. Meas. Control. 2005;127(2):218–229
11. Savaresi SM, Poussot-Vassal C, Spelta C, Sename O, Dugard L. Semi-Active Suspension Control Design for Vehicles. 2010.
12. Morselli R, Zanasi R. Control of port Hamiltonian systems by dissipative devices and its application to improve the semi-active suspension behavior'. Mechatronics. 2008;18(7):364–369.
13. Gao H, Li Z, Sun W. Energy-Driven-Damper (EDD): Comfort-Oriented Semiactive Suspensions Optimized From an Energy Perspective. IEEE Trans. Control Syst. Technol. 2020;28(5): 2069–2076.
14. Dąbrowski K. Algorytmizacja adaptacyjnego sterowania tłumieniem zawieszenia samochodu dla uwzględnienia zmienności warunków eksploatacji. 2018.
15. Koo JH, Goncalves FD, Ahmadian M. A comprehensive analysis of the response time of MR dampers. Smart Mater. Struct., 2006;15(2).

16. Krauze P, Kasprzyk J. Driving safety improved with control of magnetorheological dampers in vehicle suspension. Appl. Sci. 2020;10(24):1–29
17. Kwok NM, Ha QP, Nguyen TH, Li J, Samali B. A novel hysteretic model for magnetorheological fluid dampers and parameter identification using particle swarm optimization. Sensor and Actuators, 2006;A 132:441-451.
18. Klockiewicz Z, Ślaski G, Dąbrowski K. Simulation investigation of individual bumps recognition possibilities for damping control and possible suspension performance improvements. 2020 12th Int. Sci. Conf. Automot. SAFETY, Automot. Saf. 2020.
19. Galanti F. Modelling, Simulation, and Control for a Skyhook suspension. 2013.

Zbyszko Klockiewicz: https://orcid.org/0000-0003-4353-550X

Grzegorz Ślaski: https://orcid.org/0000-0002-6011-6625